JOURNAL OF MATERIALS SCIENCE **34** (1999) 3495–3504

Investigation of electrical conductivity of carbon black-copper phthalocyanine matrix composites

Z. ZIEMBIK, M. ZĄBKOWSKA-WACŁAWEK, W. WACŁAWEK
Opole University, ul. Oleska 48, 45-052 Opole, Poland
E-mail: waclawek@uni.opole.pl

Electrical conductivity results obtained for two component composites were measured and discussed. The composites consisted of copper phthalocyanine (semiconductor) and 7 different kinds of carbon black. The dependence of the electrical conductivity on the composite composition was examined. The percolation theory as well as the Yoshida's and McLachlan's models were utilised to describe the experimental data. The relationships between the carbon black physico-chemical properties and some parameters of the theories were found.

1. Introduction

An addition of one substance to other one gives material with new properties. For any two-component system the properties are determined by its composition, the components features and preparation conditions [1–3]. The resulting composite properties are usually intermediate in respect to the component ones, e.g. the electrical conductivity usually varies in the range limited by the values of the high- and low-conducting components. The composite fabrication is intended to improve the desired material property but often may also magnify the undesired ones [3–5]. Designing the material for certain purposes one has to take into account both possibilities. The prediction of the composite properties is usually limited only to the rough estimation [3–7]. Though the electrical conduction mechanism in composites has been outlined [8] there are still questions concerning this problem [9].

The electrically conducting composites containing carbon black are utilised in many application fields (e.g. strand shields for high voltage cables, conductive jacketing for telecommunication cables, anti-static flooring, sheeting, operating room materials, compounds for electromagnetic shielding) [6]. The influence of carbon blacks utilised as polymer fillers on the composites electrical properties have been widely discussed [5, 7, 10–12]. In this paper we would like to show and discuss electrical conductivity results obtained for carbon black (*cb*, highly conducting component), copper phthalocyanine (*Cupc*, low conducting component) composites. For the low conducting component the powdered polycrystalline organic semiconductor has been used because its physical properties are better defined than the properties of polymeric matrices usually described in the literature. In our composites one of the components, *Cupc*, remained unchanged but the second one, *cb*, was different in the various types of the materials. Our composites had small thermal conductivity and their electrical conductivity could be changed by many orders of magnitude. Their stability is high so they are expected to be good materials for possible applications. The phthalocyanine-graphite fibre composites were expected to be utilised for high temperature resistant elements in vertical and short take-off and landing aircraft [13]. We have used Yoshida's, McLachlan and percolation models to describe our experimental data. The theoretical parameters obtained from the models might be relevant to the component properties. When dependencies between the theoretical parameters and the composite characteristics exist then such relations should be helpful for the composite properties prediction.

2. Theoretical models utilised for the experimental data description

2.1. Percolation theory

Percolation theory is utilised for description of various phenomena [14]. Its application for composites conductivity considers regular or random lattices composed of conducting and non-conducting bonds. The electrical conductivity (σ) of the lattice depends on its symmetry, node co-ordination number, fraction of bonds present and distribution of the bond conductivities [14–20]. Two basic models are considered for the theoretical investigation of the electrical current flow in the lattice composed of two kinds of bonds. First of them includes the lattice composed of the bonds of $\sigma_{\text{insulator}} = 0$ and $\sigma_{\text{conductor}} > 0$ (but $\sigma_{\text{conductor}}$ is finite). The lattice bond conductivities in the second model are $\sigma_{\text{conductor}} \to \infty$ and $\sigma_{\text{dielectric}} > 0$ (but $\sigma_{\text{dielectric}}$ is finite). Electrical current can pass lattice composed of bonds posessing finite, non-zero conductivities and the insulating ones when the conducting bond fraction f is equal or exceeds the certain value called critical or percolation threshold (f_c). For this lattice $\sigma = 0$ if $f < f_c$. Close to the percolation threshold the σ dependence on f is described by the relationship:

$$\sigma \sim (f - f_c)^t \tag{1}$$

where f_c and t depend on the single bond conductivity and the lattice parameters.

The conductivity of the lattice containing the f fraction of bonds of $\sigma_{conductor} \to \infty$ and the low conducting bonds is finite for f smaller than f_c, $\sigma \to \infty$ for $f > f_c$. Conductivity of the system satisfies the relationship:

$$\sigma \sim (f_c - f)^{-s} \tag{2}$$

where f_c and s depend on the single bond finite conductivity and the lattice parameters. Taking the dimensionless, relative distance of f from f_c the relationships (1) and (2) can also written as follows [21]:

$$\sigma = c_1\{(f - f_c)/f_c\}^t \tag{3a}$$

$$\sigma = c_2\{(f_c - f)/(1 - f_c)\}^{-s} \tag{3b}$$

where c_1 and c_2 correspond to conductivities of the conductor and dielectric, respectively. Though, some materials might be superconductors in certain experimental conditions, the conductivity of a composite component are usually different from infinity. There also exist weakly conducting materials but none of them exhibits $\sigma = 0$. For the experimental data analysis the $\sigma(f)$ dependence is divided into two regions separated by f_c. For $f < f_c$ Equation 2 (or 3b) is utilised, for $f > f_c$ Equation 1 (or 3a) is valid. It is supposed, that the composite conductivity σ_{fc} for $f = f_c$ is expressed as follows [22, 23]:

$$\sigma_{fc} \sim \sigma_c^u \sigma_d^{1-u} \tag{4}$$

where σ_c, σ_d are, respectively, the conductor and dielectric conductivities, while $u = t/(t + s)$.

As mentioned above the parameters f_c, t and s depend mainly on the lattice properties. For 3D systems f_c parameter evaluated from different lattice models (site or bond percolation, mixed models) is usually limited to the range 0.16–0.18. However, other approaches to the estimation of the conductivity threshold showed that this parameter might vary from the values close to 0 up to 1/3 depending on the system investigated and method utilised [14, 15, 23–25]. The t parameter usually ranges from 1 to 3 [14, 15, 23, 25, 26]. The s exponent was found to be not smaller than 0.6 and not greater than 1.0 [22, 23, 26]. However, Kogut *et al.* [16] have shown that the t and s parameters might be greater than the supposed upper limit due to the special form of distribution of conductances in the lattice.

2.2. The Yoshida model

The Yoshida model describes the transport properties of the binary mixture [27, 28]. The real structure is approximated by the model structure composed of the four cell types (Fig. 1).

The A and B types of cells represent the regions of the material where one of the components completely surrounds the second one. Such structure is described by the Maxwell-Garnett theory [24]. The cells C and D are relevant to the composite regions where both components have the same bulk structures. The material

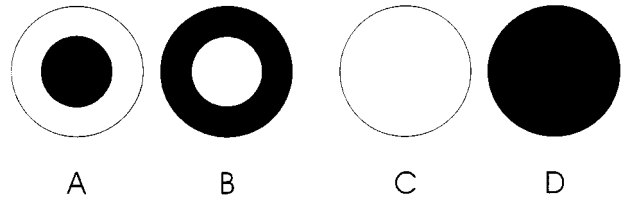

Figure 1 Four types of cells describing the material structure in the Yoshida's model.

composed of the two uniformly structured phases is described by the Bruggeman's theory [29]. The Yoshida model cells fraction depends on the materials composition and the components properties. There are six parameters describing the composite transport properties. First three of them are the component conductivities, the volume fraction of the conducting component f and the remaining three denoted as Φ, α_1, α_2 are structure related. The Φ parameter gives the volume fractions of cells C and D. The fractions F of the A, B, C and D cells are described by the following Equations:

$$F_A = (1 - \Phi)(\gamma_B - 1 + f)/(\gamma_A + \gamma_B - 1) \tag{5a}$$

$$F_B = (1 - \Phi)(\gamma_A - f)/(\gamma_A + \gamma_B - 1) \tag{5b}$$

$$F_C = \Phi f \tag{5c}$$

$$F_D = \Phi(1 - f) \tag{5d}$$

Denoting the radius of the cell K (K = A or B) as R_K and the core radius as r_K the γ_A and γ_B parameters are the ratios of $(r_A/R_A)^3$ and $(r_B/R_B)^3$, respectively. The γ_K parameters are expressed by α_1, α_2 and Φ as follows:

for $0 \le f \le \alpha_1$

$$\gamma_a = f \tag{6a}$$

$$\gamma_b = 0 \tag{6b}$$

for $\alpha_2 \le f \le \alpha_1$

$$\gamma_a = f + (3 - \alpha_1 - 2\alpha_2)[(f - \alpha_1)/(\alpha_2 - \alpha_1)]^2 + (\alpha_1 + \alpha_2 - 2)[(f - \alpha_1)/(\alpha_2 - \alpha_1)]^3 \tag{6c}$$

$$\gamma_b = 1 - f + (2\alpha_1 + 2\alpha_2)[(f - \alpha_2)/(\alpha_2 - \alpha_1)]^2 + (\alpha_1 + \alpha_2)[(f - \alpha_2)/(\alpha_2 - \alpha_1)]^3 \tag{6d}$$

for $\alpha_2 \le f \le 1$

$$\gamma_a = 0 \tag{6e}$$

$$\gamma_b = 1 - f \tag{6f}$$

Values of Φ and α_2 are limited to the ranges $\in(0, 1)$, and $\alpha_1 \le \alpha_2$. For $f > \alpha_1$ the B cells appear in the material and for $f > \alpha_2$ the cells A disappear. Fig. 2 shows an example of the changes of the cell fractions in the range from 0 to 1 for a good conductor content f (for $\Phi = 0.6$, $\alpha_1 = 0.1$ and $\alpha_2 = 0.5$). The straight lines of slope Φ and $-\Phi$ describe changes of F_C and F_D, respectively. The influence of Φ, α_1, and α_2 on the F_A and F_B fractions is shown in Fig. 3.

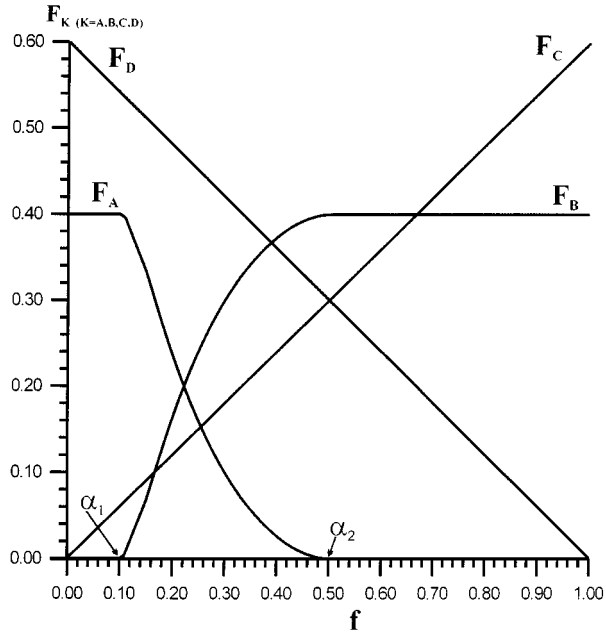

Figure 2 The changes of the K cell type fractions (K = A, B, C and D) F_K in the range from 0 to 1 of a good conductor content f (for $\Phi = 0.6$, $\alpha_1 = 0.1$ and $\alpha_2 = 0.5$).

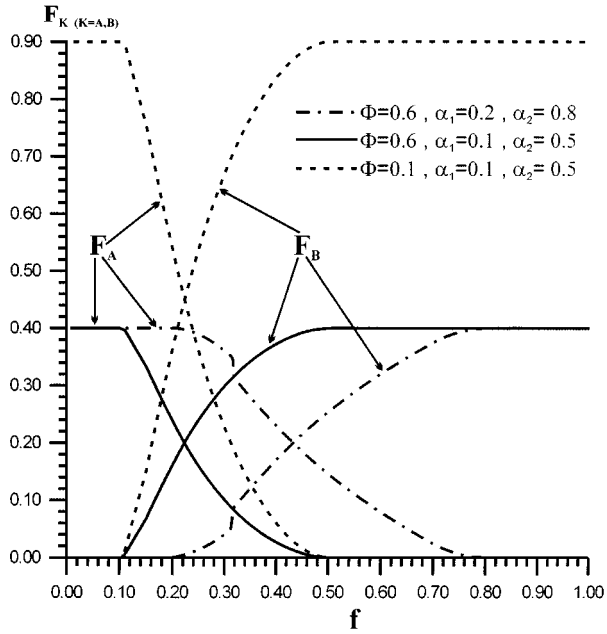

Figure 3 The changes of A and B cell types fractions in the range from 0 to 1 of a good conductor content f for various Φ, α_1 and α_2 parameters.

For $\Phi = 1$, regardless of the α_1 and α_2 values, only the cells C and D appear in the material. If $\Phi = 0$ and $\alpha_1 = \alpha_2 = 0$ (or $\alpha_1 = \alpha_2 = 1$) one of the components is represented as continuous structure containing granular inclusions of the second component.

2.3. The McLachlan model

McLachlan introduced the equation describing changes of the composite conductivity for f ranging from 0 to 1 [30–33]:

$$(1-f)\left(\sigma_d^{1/t_M} - \sigma^{1/t_M}\right)\Big/\left(\sigma_d^{1/t_M} + A\sigma^{1/t_M}\right) + f\left(\sigma_c^{1/t_M} - \sigma^{1/t_M}\right)\Big/\left(\sigma_c^{1/t_M} + A\sigma^{1/t_M}\right) = 0 \quad (6)$$

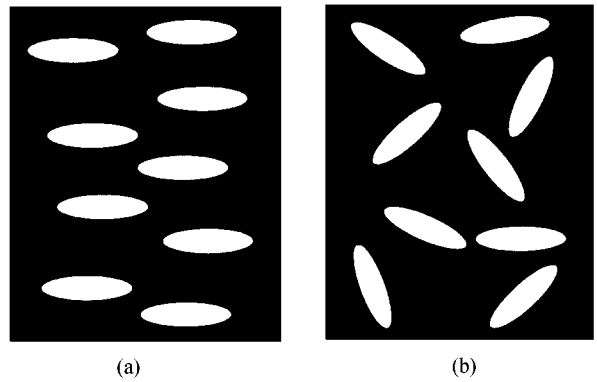

Figure 4 The model structure composed of the uniformly (a) and randomly (b) directed ellipsoids dispersed in the host material.

where $A = (1 - f_c)/f_c$, σ is the composite conductivity, σ_d and σ_c are the dielectric and conductor conductivities respectively. This relationship in its asymptotic form is reduced to percolation expressions (3a) and (3b) for zero and infinite component conductivities, respectively. In McLachlan's equation the t_M and f_c parameters are related to the other ones, describing the depolarisation coefficient of the grains in the model material. The mixture of low- or high-conducting ellipsoids of oblate or prolate shapes uniformly (Fig. 4a) or randomly (Fig. 4b) orientated in space replace the real material.

The axis ratio of the ellipsoids might be estimated from depolarisation coefficients L (high-conducting grains) or L' (low-conducting grains) for orientated ellipsoids and m, m' for random orientation respectively. If an insulator ($\sigma = 0$) is one of the composite components the following relationships are proposed [31]:

$$L' = f_c t_M^{-1} \quad (8a)$$

$$m' = t_M f_c^{-1} = 1/L' \quad (8b)$$

For the composite containing a superconducting component ($\sigma \to \infty$) the depolarisation coefficients are expressed as follows:

$$L = 1 - (1 - f_c)t_M^{-1} \quad (9a)$$

$$m = t_M(1 - f_c)^{-1} \quad (9b)$$

The above equations might be utilised for estimating the ellipsoid shape for the composites containing components that do not fulfil the assumption of the zero or infinite conductivity respectively. However, the σ_c/σ_d value should be sufficiently high to draw the proper conclusion about ellipsoid axis ratio in the composite.

3. Materials and sample preparation

In our investigations materials obtained by mixing known amounts of polycrystalline copper phthalocyanine and carbon black were used. Copper phthalocyanine is a flat molecule with macroheterocyclic ring coordinating a single copper ion (Cu^{2+}) in its centre. This compound is resistant to many chemicals and temperatures up to 200 °C. Copper phthalocyanine used in

our experiments was a deep blue powder containing α form crystallites of approx. 10 μm diameter. It was found that the electrical resistivity of Cupc used in our experiments depends on the total weight of the sample prepared. Carbon black particles are small spheroidally shaped paracrystalline unit. Interconnected particles form aggregates—discrete, colloidal entities that are the smallest dispersible units of this material. Carbon black agglomerate is comprised of a large number of aggregates physically held together.

Carbon black is characterised by particle diameters and the surface properties, which can be determined, among others, by nitrogen and dibuthyl phthalate absorption (DBPA). The distribution function of the particle diameters of the carbon black is almost normal (Gaussian) but usually positively skewed. The width of the distribution is characterised by the heterogeneity index HI defined as a ratio of the weighted mean diameter to the arithmetic mean diameter. For most commercial carbon blacks HI values for particle size range from 1.4 to 1.8 [3].

The particle diameter d (nm) and density ρ (g/cm^3) of the carbon black are related to the sepcific surface area determined by the electron microscope *EMSA* (m^2/g) *via* the following relationship:

$$EMSA = 6000/\rho d \tag{10}$$

To determine the specific surface area S of carbon black usually the BET equation is utilised with N_2 as the absorbate. The dibuthyl phthalate absorption (DBPA) parameter ν is mainly related to the aggregate shape. Absorption occurs both within the aggregate branches and between contacting aggregates in 3D network. Usually the highly branched aggregates are formed by the carbon black of high DBPA. It was found that mixing of a carbon black into a vehicle system destroys partly the aggregates structure. As the result the decrease in DBPA was observed. The new absorption value is called crushed DBPA and in this paper denoted as ν_c. The decrease in DBPA is usually significant for the *cbs* with high ν.

Carbon blacks chosen for our investigation had various physico-chemical properties such as grain diameter (d), BET specific surface area (S) and dibuthyl phthalate absorption index ν. Seven types of carbon black were utilised: Chezacarb (Czech), Jas 539, OC 2, Sakap 6 (Poland), Sapex 20 (Poland), Black Pearl 2000 and Black Pearl 700 (USA). The physico-chemical properties of carbon black used in our experiments were taken from their producers notes and are listed in Table I. There was not found any information about grain diameter of Chezacarb carbon black. We expect that the relationship between S and d would have been similar to inverse proportionality in Equation 10. Fig. 5 shows the dependence d vs. $1/S$ found for a number of different carbon blacks (most of them were Cabot Corp. products).

Good interpolation of d vs. $1/S$ was obtained with polynomial fit of the of third order (with correlation coefficient $r = 0.9683$). The estimated particle size of Chezacarb was 15.4 nm.

TABLE I Grain diameter d, specific surface area S and dibuthyl phthalate absorption index ν of the carbon blacks used for the composites preparation

Carbon black	d (nm)	S (m^2/g)	ν (cm^3/100 g)
Black pearl 2000	15	1475	330
Black pearl 700	18	200	117
Chezacarb	15.4 (estim.)	1000	370
Jas 539	45	47	95
OC 2	26	100	100
Sakap 6	25	200	120
Sapex 20	70	20	86

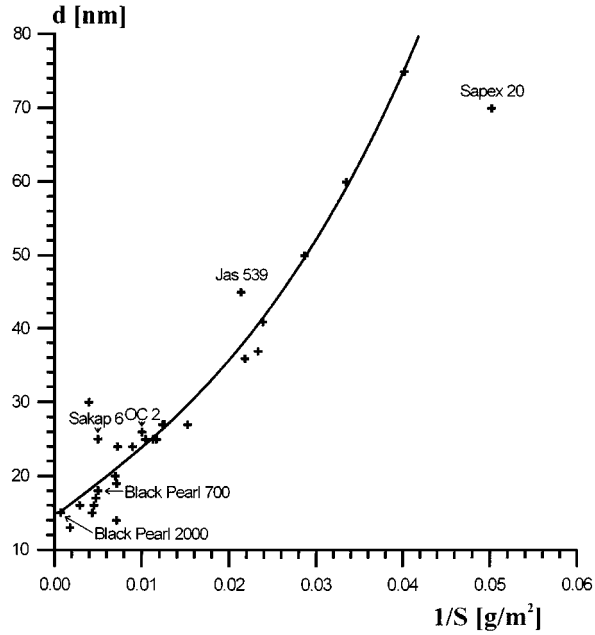

Figure 5 The relationship between the inverse BET surface area S and the grain diameter d of carbon blacks.

Two kinds of methods of the composite preparation were utilised. First of them involved homogenisation of the mixture by grinding the known amounts of *cb* and *Cupc* in the agalite mortar. The preliminary data analysis has shown that the electrical conductivity of the composite depends on the amount of the mixture ground in the mortar (especially for low *cb* concentrations). To examine this effect the total weight of the material ground was chosen to be 1, 4 or 10 g. To avoid mechanical stress during the homogenisation other method of preparation was utilised. Vesselus containing liquid suspension of Black Pearl 700 and *Cupc* in acetone were placed in the ultrasound bath for 20 min. Neither *Cupc* nor the carbon black was soluble in acetone. No significant influence of homogenisation time (within 10–60 min) on the electrical properties of the mixture was observed. The material obtained was dried by heating in 150 °C for 5 h and kept in vacuum (approx. 0.1 Pa) for two days. Portions (0.25 g) of the materials obtained by the above-described procedures were compressed to obtain pellets of 10 mm in diameter and 2 mm thick. In this paper the composite names contain parts denoting the carbon black type and the weight of material prepared, e.g. BP7-4 is the composite containing Black Pearl 700

and the amount of the mixture ground in mortar was 4 g. The composite BP7-u was obtained by homogenisation in an ultrasound bath.

To improve the electrical contact between the electrode and the sample both surfaces were covered by silver paint. The electrical conductivity of the pellets in three heating-cooling cycles remained unchanged. This result suggests absence of silver diffusion into the material or at least no influence of this effect on the DC conductivity of the pellets. For the BP7-u composite the stability of the components pre-treated in acetone and then dried should also be noted. The conductivity measurements were carried out at room temperature using Keithley 197 and Keithley 195A multimeters.

4. Results and discussion

Figs 6 and 7 show the $\log(\sigma)$ vs. f dependencies for the composites investigated. The solid and dashed lines show the computed best fit for the McLachlan's and Yoshida's models, respectively.

The parameters computed were f_c, t_M for the McLachlan model and Φ, α_1, α_2 for the Yoshida's model. The inflection points of the experimental $\log(\sigma)$ vs. f plots were used for f_c estimation. Conductivities for the both composite components were also computed. Due to the *cb*'s properties the direct measurement of bulk conductivity σ_{cb} was impossible for the pelletised form—after compaction the pellets broke into pieces immediately. Because of that σ_{cb} was obtained as a fitted parameter. The *Cupc*'s bulk conductivity (σ_{pc}) was established for a pellet but in the computations some variation of its value was allowed to obtain the best fit. The results obtained for McLachlan's equation are shown in Table II.

Janzen introduced the relationship between the ν index characterising the aggregate structure, the *cb*'s density and the critical volume fraction f_c^J of *cb* in composites [3]. This formula is presented below:

$$f_c^J = (1 + 4\rho\nu)^{-1} \tag{11}$$

where ρ is *cb*'s density in g/cm^3 and ν values are in cm^3/g. The pycnometric density of various carbon blacks in benzene was found to be approximately within the range of 1.8–2.0 g/cm^3 [3]. Taking the average ρ value of 1.9 g/cm^3 and $\Delta\rho = \pm 0.1$ g/cm^3 as the density uncertainty the expected values of f_c^J and the $\Delta\rho$-caused deviations (Δf_c^J) were computed. The results obtained are shown in Table III.

The results in Table III show that the Janzen formula predicted properly the f_c value for the Chez-10, BP2-4, and Sap-1 composites. The difference between the f_c values found for BP7-u and computed from Equation 11 exceeds the predicted Δf_c^J. However, due to the unknown ν error of Black Pearl 700 and the low relative f_c deviation value $100\% * (f_c - f_c^J)/f_c = 7.3\%$ the fair agreement of f_c and f_c^J values is supposed. The differences found for the other composites were significant.

TABLE II The f_c, t_M, σ_{cb} and σ_{pc} parameters found for the composites investigated

Composite type	f_c	t_M	$\sigma_{cb} \times 10^{-2}$ (S/m)	$\sigma_{pc} \times 10^{-7}$ (S/m)
BP2-4	0.0394	2.77	20	0.78
BP7-4	0.0698	1.76	2.7	0.72
BP7-u	0.109	1.24	0.28	19
Chez-1	0.0798	1.37	6.3	47
Chez-10	0.0344	2.25	58	0.20
Jas-1	0.170	1.55	3.4	22
OC-1	0.165	1.22	2.4	8.2
Sak-1	0.241	1.58	0.79	31
Sak-4	0.204	1.65	7.0	3.3
Sap-1	0.135	1.93	9.3	4.9

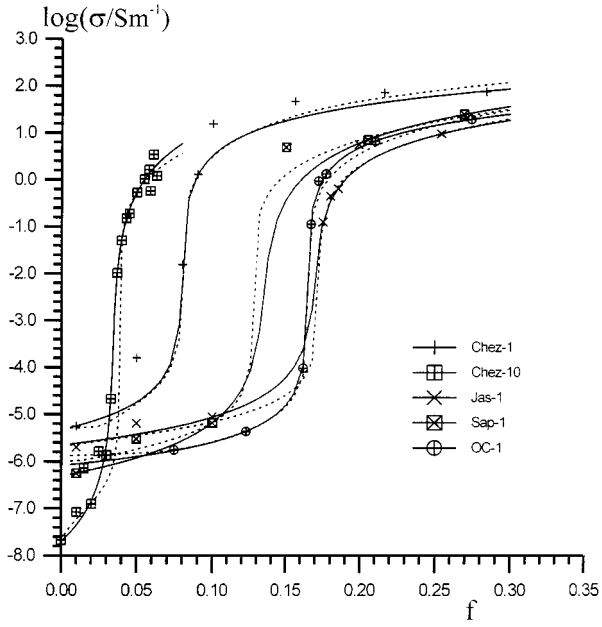

Figure 7 The dependence of the logarithm of the composites electrical conductivity on *cb* content f. Solid and dashed lines represent the plots of the best fit found for the McLachlan's and Yoshida's models respectively.

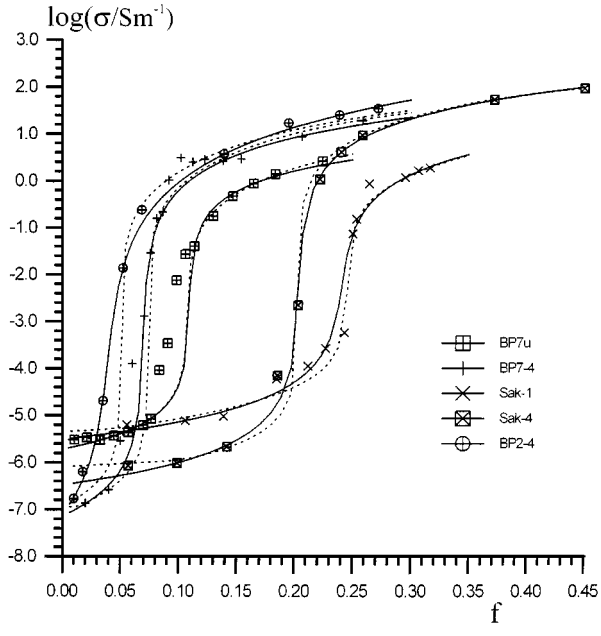

Figure 6 The dependence of the logarithm of the composites electrical conductivity on *cb* content f. Solid and dashed lines represent the plots of the best fit found for the McLachlan's and Yoshida's models respectively.

TABLE III The computed f_c^J values, the differences between the experimentally estimated f_c (Table II) and the f_c^J found from Janzen equation, and the computed Δf_c^J values for the investigated *cb*s in the composites

Composite type	f_c^J	$(f_c - f_c^J) \times 10^3$	$\Delta f_c^J \times 10^3$
BP2-4	0.0383	1.1	1.9
BP7-4	0.101	−31.2	4.8
BP7-u	0.101	8	4.8
Chez-1	0.0344	46	1.9
Chez-10	0.0344	0.0	1.9
Jas-1	0.122	48	5.6
OC-1	0.116	49	5.4
Sak-1	0.0988	142	4.7
Sak-4	0.0988	105	4.7
Sap-1	0.133	2	6.1

With exception of BP7-4 composite the f_c values found experimentally were higher than f_c^J computed from Equation 11. Higher than expected values of f_c suggest the decrease in the DBPA values after grinding in mortar. The ν index is related to the structure of *cb* aggregates. During the composite preparation these aggregates were probably crushed because of this the initial *cb* properties described by ν were changed in the final material.

Excluding Sap-1 the greatest difference between f_c and f_c^J was observed for the composites prepared from 1 g mixtures. As the result of the small amount of both materials the layer between the mortar and the pestle was thinner for 1 g mixtures than for 4 and 10 g ones. The destruction of *cb* aggregates was more efficient for 1 g mixtures than for the greater quantities of the ground material. Because of the good agreement between f_c and f_c^J found for Sapex 20 *cb* it might be concluded that this aggregates were the most resistant to mechanical stress while grinding. The greatest sensitivity on mechanical crushing of aggregates was observed for the Sakap 6 carbon black. For both 1 and 4 g batches of the Sakap 6 mixtures the deviations from f_c^J values were the greatest among the samples tested. Utilising Equation 11 and the f_c values obtained for our composites the estimation of ν_c values was computed. The ν_c parameters and the differences $\nu - \nu_c$ are collected in Table IV.

With an exception of the BP7-4 composite for the other materials investigated there was suggested the decrease in DBPA as the result of mechanical treatment. The difference $\nu - \nu_c$ might be taken as a measure of the *cb* agglomerate destruction during the composite preparation. However, while it might be envisaged that the Chezacarb *cb* was the most easily to crush while grinding (Chez-1) it should be noticed that practically no influence on the aggregate structure was observed for the larger amounts of the mixture ground (Chez-10). The Sapex 20 aggregates appeared to be the most resistant to the mechanical stress. The data in Table IV confirm the supposition that there exists relation between the mixtures weights taken for grinding and the conducting clusters structure in the composite obtained. For BP7-4 there was observed the increase in the estimated DBP absorption. This observation is an exemption from the other materials and might be the result of the specific Black Pearl 700 structure and mechanical properties of the *cb* aggregate. For this *cb* the grinding procedure might not only destroy the aggregates but also rejoin them together again. As the result the higher than expected composite conductivity was observed.

There was found the relationship between f_c and the *cb* grain diameter. The threshold volume fraction increases while the grain diameter d grows. According to the Kusy's model [34] the f_c value for a composite consisting of spherical grains of two components depends on their diameter ratio. It was shown that f_c is inversely proportional to the linear function of the $d_{\text{dielectric}}/d_{\text{conductor}}$ ratio. Fig. 8 shows the relationship between d^{-1} and f_c.

The statistical parameters of this linear relationship as well as the parameters of the dependencies discussed further are collected in Table VIII. Excluding the points representing the *cbs* with the greatest grain diameters i.e. Jas 539 and Sapex 20, the line obtained from the Kusy's model describes the positions of the remaining ones well. Assuming small changes of the *pc*'s grain diameters in the composites, the crucial role of the *cb*'s

TABLE IV The dibuthyl phthalate absorption indexes ν of the carbon blacks, the estimated ν_c found for the composites investigated and the differences $\nu - \nu_c$

Composite type	ν (cm^3/100 g)	ν_c (cm^3/100 g)	$\nu - \nu_c$ (cm^3/100 g)
BP2-4	330	321	9
BP7-4	117	175	−58
BP7-u	117	108	9
Chez-1	370	152	218
Chez-10	370	369	1
Jas-1	95	64	31
OC-1	100	67	33
Sak-1	120	41	79
Sak-4	120	51	69
Sap-1	86	84	2

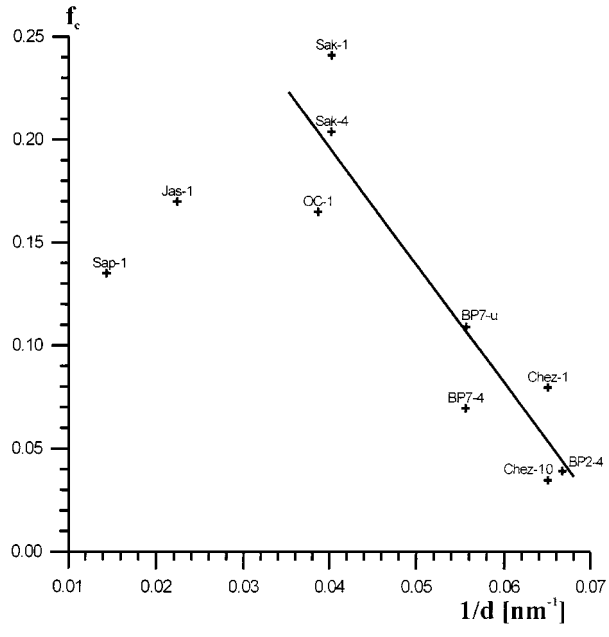

Figure 8 The relationship between the threshold volume fraction f_c and the inverse grain diameter d^{-1} of the investigated *cb*s.

grain diameter in defining the conducting cluster (agglomerate) size might be concluded. This supposition is also supported by the results obtained by Wacławek *et al.* [35] who observed for the phthalocyanine - carbon black composites containing 20% of *cb*, the decrease in the electrical conductivity with increasing grain diameters.

The extrapolated conductivities of carbon black σ_{cb} depended not only on the *cb* type but also on the preparation conditions. The increase in weights of the mixtures ground was followed by increase in the *cb* conductivity (Chezacarb, Sakap 6). For Black Pearl 700 there was observed the decrease in σ_{cb} related to the change of the preparation method. The decrease in σ_{cb}—in spite of the soft homogenising—method (ultrasonic bath) was probably due to the changes of the *cb* aggregate surface properties. It is possible that acetone, utilised as the suspensing medium, removed from the *pc* microcrystallites some impurities which were then absorbed on the *cb* aggregates surface. As a result of the surface coverage the electrical contact between aggregates became poor and the decrease in conductivity of the *cb* network was observed.

The changes of σ_{pc} for different composites proved the influence of the microcrystallite contact on the averaged conductivity of the phthalocyanine matrix. For small amounts of the mixtures ground in a mortar the surfaces of copper phthalocyanine microcrystallites were efficiently pressed against each other. The formation of the interface connection might be affected also by the *cb* mechanical properties. However, the origin of the main influence on *pc*'s conductivity should be related to the conditions facilitating the intergrain contact, e.g. the pressure applied on the material while grinding which, in turn, depends on the total weight of the mixture. The second factor influencing the *pc* conductivity is temperature. The measurements were performed at room temperature, which can fluctuate in some narrow range. Thus, changes in phthalocyanine matrix conductivity with temperature might be expected due to the thermally activated conduction of *pc*.

Table V contains the computed depolarisation coefficients L and m of the ellipsoids representing *cb* and *pc* in the material. As it was proposed by McLachlan [31] the depolarisation coefficient values allow estimating the shapes and axis ratios of ellipsoids in the model material. The x parameter is defined as the ratio of the c axis of the ellipsoid to the a axis ($c = b \neq a$). The x values in Table were estimated from the plot shown in [31].

TABLE V The depolarisation coefficients found for the ellipsoids representing carbon black and copper phthalocyanine in the composites and corresponding axis ratios

Composite type	L_{cb}	m_{cb}	L_{pc}	m_{pc}	x_{cb}	x_{pc}
BP2-4	0.0142	70.4	0.653	2.88	>10	<0.1
BP7-4	0.0397	25.2	0.472	1.89	>10	~0.33
BP7-u	0.0876	11.4	0.281	1.39	>10	~1
Chez-1	0.0583	17.1	0.328	1.49	>10	~1
Chez-10	0.0876	11.4	0.281	1.39	~10	~1
Jas-1	0.110	9.09	0.468	1.87	5–10	~0.33
OC-1	0.135	7.41	0.316	1.46	6–4	~1
Sak-1	0.153	6.53	0.520	2.08	4–5	~0.1
Sak-4	0.124	8.06	0.518	2.07	5–6	~0.1
Sap-1	0.0700	14.3	0.552	2.23	>10	~0.1

The x_{cb} parameters show that oblate grains in the model composite represent the carbon black aggregates. The most flat is the ellipsoid corresponding to Black Pearl 2000, Black Pearl 700, Chezacarb and Sapex 20 *cbs* in the composite. The Jas 539 is represented by the ellipsoids of the approximate axis ratio 7 : 1. The Sakap 6 and OC 2 carbon blacks might be described by similar ellipsoidal structures with the axis ratio within the range from 4 : 1 to 6 : 1. It was expected that the grains of copper phthalocyanine in real material would be similar in all composites. For Chez-1, OC-1 and BP7u composites the *cupc* grains were nearly spherical. For the other composites investigated the *pc* corresponding grains were oblate with approximate axis ratio 1 : 3 (Jas-1, BP7-4) and 1 : 10 (Sak-1, Sak-4, Sap-1). The *pc* in BP2-4 is best described as strongly elongated, rodlike structures of axis ratio $1 : y$, with y exceeding 10.

The relationship between the depolarisation coefficients found for *cbs* and the grain diameters were observed. If d was not greater than approx. 30 nm the linear increase in L_{cb} with increasing grain diameter was found (Fig. 9). It might be expected that the *cb* conducting cluster features were influenced by the *cb* grain diameter d what affected the final electrical properties of the composite.

Fig. 10 shows the plot of the $\log(m_{cb})$ depolarisation coefficient dependence as a function of the estimated ν_c parameter value. Though, both m_{cb} and ν_c share the f_c dependence (Equations 8a and 8b), the m_{cb} parameter was also determined by the t_M variable that makes the $m_{cb}(\nu_c)$ relationship not so obvious. Although in this paper the ν_c parameters have been merely estimated, the relationship $\log(m_{cb})$ vs. ν_c found points at usefulness of ν_c in the composite properties assessing.

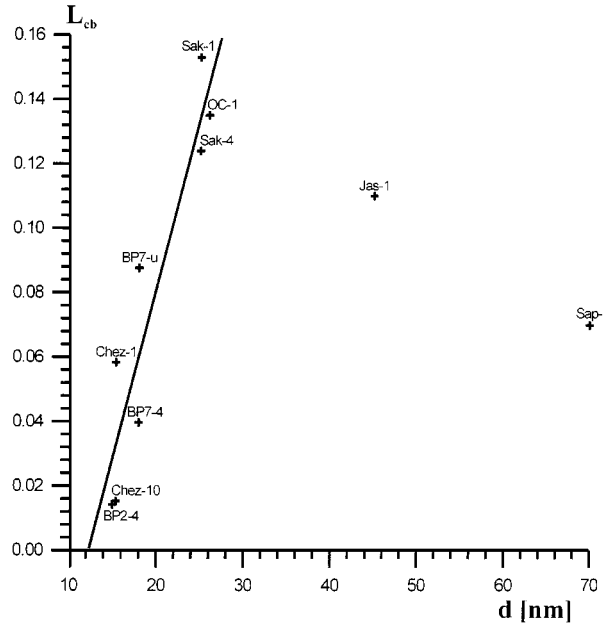

Figure 9 The depolarisation coefficient L_{cb} dependence on the *cb*'s grain diameter d.

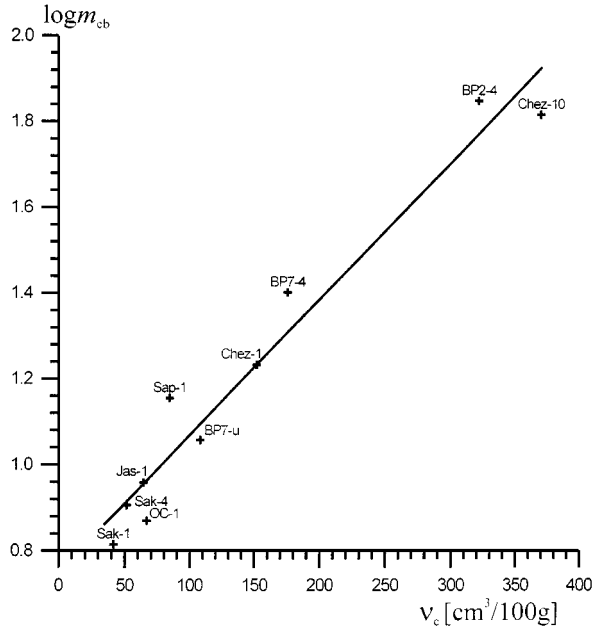

Figure 10 The logarithm of m_{cb} dependence on the estimated ν_c of the investigated *cb*s.

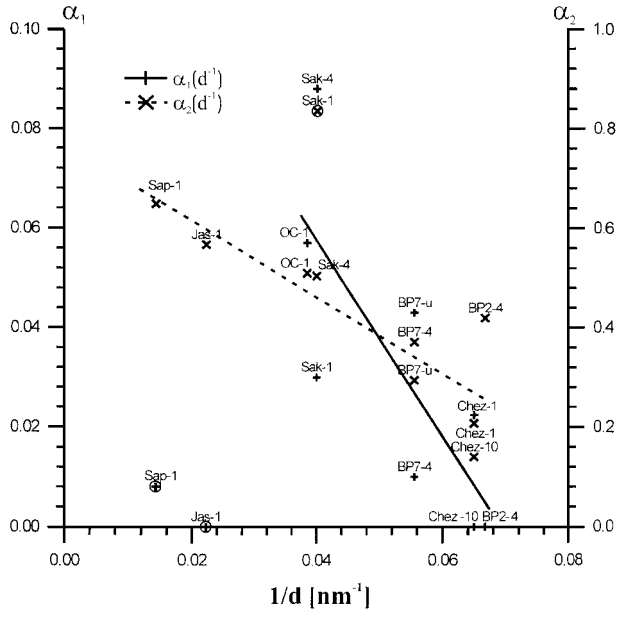

Figure 11 The α_2 and α_2 parameters dependence on the inverse grain diameter d^{-1} of the investigated *cb*s. The points in circles were excluded from computations.

Table VI presents the results obtained from application of the Yoshida's model to our results. The lowest Φ value was found for the Sak-1 composite. These results suggest the prevalence of the structure shown on Fig. 1a where the phases surround each other. The highest Φ was found for the composites containing Jas 539 and Chezacarb *cbs*. For this materials the fraction of the structures shown on Fig. 1c, d is the highest among the materials investigated. A decrease in the value of the difference $\alpha_2 - \alpha_1$ with increasing Φ can be seen. This implies narrowing of the f range where the cells A and B coexist. The α_1 values change in range not exceeding 0.1 and the α_2 parameter varies more than 0.6. It might be expected that α_1 is influenced primary by the low-conducting component properties that in our composites were not changed. The α_2 parameter, which values varied within a broader range, might characterise the high-conducting component i.e. the different types of carbon black. Fig. 11 shows the d^{-1} dependence of α_1 and α_2. Excluding the points representing the *cbs* of the greatest grain diameters (i.e. Jas 539 and Sapex 20) the remaining ones are expected to be linearly dependent on d^{-1}.

TABLE VI The Φ, α_1, α_2, σ_{cb} and σ_{pc} parameters found for the composites investigated

Composite type	Φ	α_1	α_2	$\sigma_{cb} \times 10^{-2}$ (S/m)	$\sigma_{pc} \times 10^7$ (S/m)
BP2-4	0.243	0.000	0.419	2.0	1.1
BP7-4	0.442	0.010	0.371	2.0	1.1
BP7-u	0.577	0.043	0.294	0.44	30
Chez-1	0.656	0.022	0.207	11	50
Chez-10	0.650	0.000	0.146	8.5	0.21
Jas-1	0.636	0.000	0.567	3.0	21
OC-1	0.405	0.057	0.510	3.6	13
Sak-1	0.030	0.030	0.836	0.95	45
Sak-4	0.512[a]	0.088[a]	0.504[a]	3.5	8.1
Sap-1	0.144	0.008	0.649	4.2	10

[a]This result is taken from [36].

Similar relationship was introduced for the α_2 vs. d^{-1} plot where the point representing the Sak-1 composite should be omitted. Since the number of grains in 1D chain of a given length is inversely proportional to their diameter the conclusion is that the dependence of α_1 and α_2 parameters on d^{-1} involves the processes on the contacting grain surfaces.

Percolation theory is expected to describe the composite conductivity close to percolation threshold i.e. for f not very different from f_c. To obtain the parameters t, c_1, s and c_2 from the percolation Equations 3a and b, the slope and the intercept of log σ vs. log$(f - f_c)$ and log σ vs. log$\{(f_c - f)/f_c\}$ plots in their linear part were computed. The results are shown in Table VII.

It was found that the $\sigma(f)$ relationship for the composites containing Sapex 20 did not satisfy the percolation theory equations. For the other composites the threshold volume fraction f_c shown in Table III and t, s exponents (Table V) are comparable to the values predicted by the percolation theoretical models. The higher than expected values of the s parameter (i.e. $s \sim 0.7$) were found for most of the composites. This fact might be explained by the model proposed by Kogut *et al.* [16]

TABLE VII The t, s, c_1 and c_2 parameters found for the investigated composites

Composite type	t	s	c_1 (S/m)	$c_2 \times 10^7$ (S/m)
BP2-4	2.6	2.3	0.45	1.1
BP7-4	1.7	4.3	4.3	0.15
BP7u	2.2	0.58	1.8	23
Chez-1	4.2[a]	—	2.2×10^3	—
Chez-10	2.2	1.9	2.8	0.53
Jas-1	1.6[a]	1.7	46	26
OC-1	1.5[a]	0.88	42	12
Sak-1	1.1[a]	1.6	21	39
Sak-4	1.7	1.5	67	5.4

[a]The data are taken from [37].

TABLE VIII The values of the slope a, the intercept b and standard deviations s_a, s_b of this parameters, the correlation coefficient r and its confidence level α

Relationship	Points excluded	a	s_a	b	s_b	r	α
$f_c(1/d)$	Sap-1, Jas-1	−6	1	0.43	0.05	−0.925	0.999
$L_{cb}(d)$	Sap-1, Jas-1	0.011	0.002	−0.13	0.03	0.929	0.999
$\log m_{cb}(\nu_c)$	—	0.0032	0.0003	0.75	0.05	0.976	1.000
$\alpha_1(1/d)$	Sap-1, Jas-1	−2.0	0.6	0.14	0.03	−0.783	0.978
$\alpha_2(1/d)$	Sak-1	−8	2	0.77	0.08	−0.873	0.998
$t(1/d)$	Jas-1, Chez-1	35	9	0.02	0.49	0.861	0.987
$\log c_1(1/d)$	Jas-1, Chez-1	−61	11	4.0	0.6	−0.932	0.998

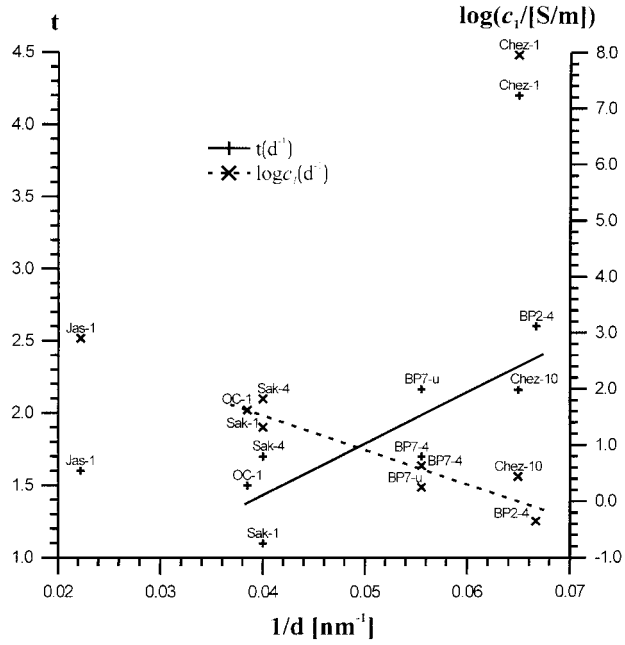

Figure 12 The t exponent and log c_1 dependence on the inverse grain diameter d^{-1} of the investigated *cb*s.

involving the specific form of the distribution function of conductances. The relationship between the parameters from Equations 3a and b, was proposed by Kirkpatrick [38]:

$$s/t = f_c/(1 - f_c) \tag{12}$$

However, the above relationship is not satisfied by the parameters found in our experiment. An increase in the t exponent with the decreasing grain diameter d was observed. Fig. 12 shows the t vs. d^{-1} and log c_1 vs. d^{-1} dependencies.

The point representing the Chez-1 composite is visibly different than the others. Furthermore, the composite containing Jas 539 *cb* also does not fall into the straight line defined by the locations of all other points on the plot. Similarly, the linear relationship with the same exceptions was found for log c_1 vs. d^{-1} plot. The c_1 increase with increasing d suggests that the *cb* cluster conductivity is limited by the conductivities of contacts between the adjacent grains. No reliable relationships were found between the s exponent as well as the c_2 parameter and the *cb*'s properties shown in Table I.

The c_1 and c_2 parameters should be discussed in relation to the σ_{cb} and σ_{pc} conductivities found by utilising the McLachlan's and Yoshida's models. For the composite the corresponding conductivities of its components were similar, independently on the model applied. σ_{cb} of order 10^2 S/m is usually reported for bulk *cb*'s and this is comparable to our results. The c_1 parameter varied in the range 10^{-3} to 10^1 S/m and was lower than σ_{cb}—in contrast to the c_2 parameter which values were similar to the computed values of σ_{cb}. These results shows the difference between the electrical conductivity of the bulk *cb* and the same property of the cluster composed of the *cb* grains dispersed in the *pc* matrix. The parameters from the McLachlan's and Yoshida's models discussed earlier were utilised for $\sigma(f)$ description in the whole range of fractions investigated. This is in contrast to the percolation description, limited to the relatively narrow range of f close to the f_c value.

The statistical parameters of the linear relationships $y(x) = ax + b$ found for our composites are collected in Table VIII. The first column in Table VIII contains the description of the relationship and the second column includes information about the points excluded from computations. The parameters s_a and s_b are the standard deviations of the slope a and the intercept b, respectively. The last column in Table VIII contains the computed values of the confidence level α of the correlation coefficient r.

5. Conclusions

The conductivity dependence on the volume fraction of *cbs* content was quite well described by the McLachlan and Yoshida models as well as the equations derived from the percolation theory (with the exception of the composites containing Sapex 20 *cb*). Several relationships between the physico-chemical properties of *cbs* and the parameters from the models were found.

In the composite preparation the *cb* aggregate structures were probably changed enough to lose its primary properties characterised by the DBPA index value. For the composites containing the same carbon black (Sakap 6 in Sak-1 and Sak-4, Chezacarb in Chez-1 and Chez-10) but prepared using the different amounts of the material for a mortar grounding, the influence of the total weight of the mixture on most of the parameters investigated was observed. As a result the *cb*'s aggregates were broken into pieces and smaller amounts of the grainy material in the mortar were easier to crush than the larger ones. The Janzen's formula allows predicting the f_c values of the composites obtained utilising the mixing methods that did not fracture the *cb* aggregates extensively. It was expected that for BP7-4

the mixing procedure caused additional tangling of the *cb* aggregates resulting in the decrease in f_c and the subsequent increase in DBPA. For the other composites f_c values lower than predicted by the Janzen's formula were found.

The most characteristic for our composites was the crucial role of the grain diameter and the intergrain contacts in the theoretical parameter determination. The number of contacts between the grains in 1D chain (proportional to d^{-1}) affects the threshold volume fraction f_c, α_1 and α_2 parameters of the Yoshida model as well as the t exponent and c_1 parameter from percolation theory. However, the exceptions from these relations were found, especially in the case of the Chez-1 composite for the $f_c(d^{-1})$, $t(d^{-1})$ and $\log c_1$ vs. d^{-1} relationships. The comparison of ν and the estimated ν_c values obtained for Chez-1 suggests a very significant damage to the *cb* aggregates during the preparation procedure. The observed deviations of the parameters characterising Chez-1 from the theoretical relationships might be caused by such *cb* aggregates fracture. For the *cbs* possessing the greatest grain diameters (i.e. Jas 539 and Sapex 20) the deviations from the outlined formulas were found for the α_1 vs. d^{-1}, t vs. d^{-1}, $\log c_1$ vs. d^{-1} and L_{cb} vs. d relationships. From the (approximately) inverse proportionality of α_2 and d falls out the point representing the Sak-1 composite. For all of the composites investigated there was found exponential relationship between the depolarisation coefficient of the randomly orientated, conducting ellipsoids (m_{cb}) and ν_c parameter estimated from the Janzen's formula.

Although, there were found few exceptions it was shown that some of the parameters describing the composite conductivity were predictable on the basis of the components properties at least within the specified class of materials (the *pc-cb* system was described). Designing of composite properties might be supported and simplified using the parameters from the selected theories to obtain the materials with predicted properties in the simple and cheap way.

References

1. Technical Report S-39, Cabot Corp.
2. M. NARKIS, R. TCHOUDAKOV and A. SIEGMANN, in Proceedings of the Second Conference on Carbon Black, Mulhouse (F), 27–30 Sept. 1993, p. 231.
3. J. -B. DONNET, R. CH. BANSAL and M. -J. WANG, "Carbon Black. Science and Technology" (Marcel Dekker, New York, Basel, Hong Kong, 1993).
4. R. A. SWOR, D. R. HARRIS and F. LYON, *Kautsch., Gummi, Kunstst.* **37** (1984) 198.
5. F. GUBBELS, S. BLACHER, E. VANLATHEM, R. JÉRÔME, R. DELTOUR, F. BROUERS and PH. TEYSSIÉ, *Macromolecules* **28** (1995) 1559.
6. Technical Report S-34, Cabot Corp.
7. J. R. NELSON and W. K. WISSING, *Carbon* **24** (1986) 115.
8. A. KOŁEK, *Int. J. Electron.* **76** (1994) 1043.
9. J. C. DAWSON and C. J. ADKINS, *J. Phys: Condens. Matter* **8** (1996) 8321.
10. R. A. SWOR, D. R. HARRIS and F. LYON, *Kautsch. Gummi Kunststoffe* **37** (1984) 198.
11. J. H. KAISER, *Appl. Phys. A* **56** (1993) 299.
12. C. BROSSEAU, F. BOULIC, P. QUEFFELEC, C. BOURBIGOT, Y. LEMEST, J. LOAEC and A. BEROUAL, *J. Appl. Phys.* **81** (1997) 882.
13. R. Y. TING, in "Advanced Composites; Design and Applications MFPG," 29th Meeting (NBS Special Publication) p. 563.
14. R. ZALLEN, "The Physics of Amorphous Solids" (John Wiley and Sons, 1983).
15. S. KIRKPATRICK, *Phys. Rev. Lett.* **36** (1976) 69.
16. P. M. KOGUT and J. P. STRALEY, *J. Phys. C: Solid State Phys.* **12** (1979) 2151.
17. M. SAHIMI, *ibid.* **19** (1986) 1311.
18. J. AXEL and G. GRIMVALL, *ibid.* **21** (1988) L47.
19. J. SCHMITTBUHL, G. OLIVIER and S. ROUX, *J. Phys. A: Math. Gen.* **25** (1992) 2119.
20. M. PERREAU, J. PEIRO and S. BERTHIER, *Phys. Rev. E* **54** (1996) 4590.
21. M. A. DUBSON and J. C. GARLAND, *Phys. Rev. B* **32** (1985) 7621.
22. I. WEBMAN, J. JORTNER M. and M. H. COHEN, *ibid.* **16** (1977) 2593.
23. M. A. J. MICHELS, *J. Phys: Condens. Matter* **4** (1992) 3961.
24. F. BROUERS, *J. Phys. C: Solid State Phys.* **19** (1986) 2151.
25. M. P. HOLLEWAND and L. F. GLADDEN, *J. Phys: Condens. Matter* **4** (1992) 5757.
26. F. BROUERS and A. RAMSAMUGH, *J. Phys. C: Solid State Phys.* **21** (1988) 1839.
27. K. YOSHIDA, *Phil. Mag. B* **53** (1986) 55.
28. *Idem., J. Phys. Soc. Jap.* **59** (1990) 4087.
29. R. LANDAUER, *J. Appl. Phys.* **23** (1952) 779.
30. D. S. MCLACHLAN, *Sol. State Comm.* **60** (1986) 821.
31. *Idem., J. Phys. C: Solid State Phys.* **20** (1987) 865.
32. *Idem., J. Appl. Phys.* **68** (1990) 195.
33. D. S. MCLACHLAN, M. BLASZKIEWICZ and R. E. NEWNHAM, *J. Amer. Ceram. Soc.* **73** (1990) 2187.
34. R. P. KUSY, *J. Appl. Phys.* **48** (1977) 5301.
35. W. WACŁAWEK and M. ZĄBKOWSKA-WAC ŁAWEK, *J. Mater. Sci. Lett.* **6** (1987) 784.
36. R. PIASECKI, Z. ZIEMBIK, W. WACŁAWEK and M. ZĄBKOWSKA-WACŁAWEK, *Phys. Stat. Sol. (a)* **123** (1991) K145.
37. Z. ZIEMBIK, M. ZĄBKOWSKA-WACŁAWEK and W. WACŁAWEK, *ibid.* **124** (1991) K123.
38. S. KIRKPATRICK, *Phys. Rev. B* **15** (1977) 1533.

Received 9 January 1998
and accepted 27 January 1999